

Measurement of the cross-section ratio ${}^3\text{H}(d,\gamma){}^5\text{He}/{}^3\text{H}(d,\alpha)n$ at 100 keV

J. E. Kammeraad, J. Hall, and K. E. Sale

Lawrence Livermore National Laboratory, Livermore, California 94550

C. A. Barnes, S. E. Kellogg,* and T. R. Wang†

W. K. Kellogg Radiation Laboratory, California Institute of Technology, Pasadena, California 91125

(Received 16 January 1992; revised manuscript received 29 September 1992)

The cross-section ratio for ${}^3\text{H}(d,\gamma){}^5\text{He}$ relative to ${}^3\text{H}(d,\alpha)n$ has been measured at an effective deuteron bombarding energy of 100 keV with a NaI pair spectrometer and a tritiated-titanium target. The ratio was determined to be $(1.2 \pm 0.3) \times 10^{-4}$ by comparing the spectra and count rates for ${}^3\text{H}(d,\gamma){}^5\text{He}$ and ${}^3\text{H}(d,\alpha)n$ with ${}^2\text{H}({}^3\text{He},\gamma){}^5\text{Li}$ and ${}^2\text{H}({}^3\text{He},\alpha){}^1\text{H}$.

PACS number(s): 25.45.-z, 27.10.+h, 25.10.+s

I. INTRODUCTION

Measurements of the cross-section ratio for ${}^3\text{H}(d,\gamma){}^5\text{He}$ relative to ${}^3\text{H}(d,\alpha)n$ are needed if gamma rays from ${}^3\text{H}(d,\gamma){}^5\text{He}$ are to be used as a monitor for ${}^3\text{H}(d,\alpha)n$ "fusion" reactions. Prior to 1984, the existing measurements [3–6] in the energy region of interest (near $E_d = 107$ keV) were statistically inconsistent and covered a range of a factor of 30. This situation motivated the present experiment and two other recent experiments: Cecil and Wilkinson [1] measured $(5.4 \pm 1.3) \times 10^{-5}$, and Morgan *et al.* [2] measured $(5.6 \pm 0.6) \times 10^{-5}$. In addition to these "branching-ratio" experiments, measurements of the cross section for ${}^3\text{H}(d,\gamma){}^5\text{He}$ were made by Batay-Csorba and Barnes [7] for $E_d = 2$ –12 MeV, and measurements of the cross section and analyzing powers $A_y(\theta)$ and $A_{yy}(\theta)$ were made by Riley, Weller, and Tilley [8].

In the present experiment, the gamma rays from ${}^3\text{H}(d,\gamma){}^5\text{He}$ and ${}^2\text{H}({}^3\text{He},\gamma){}^5\text{Li}$ were measured with a pair spectrometer. The energy-level structures of ${}^5\text{He}$ and ${}^5\text{Li}$ are essentially the same for the ground states and first two excited states [9], as should be expected for these mirror nuclei. On the basis of the charge independence of the nuclear force, it is reasonable to assume that the gamma-ray spectra for decays from the second excited states in these nuclei will also be very similar. We therefore measured the gamma rays from these two reactions with the same experimental apparatus and techniques, and analyzed the measurements with the same peak shapes. Since the cross-section ratio for ${}^2\text{H}({}^3\text{He},\gamma){}^5\text{Li}$ relative to ${}^2\text{H}({}^3\text{He},\alpha){}^1\text{H}$ is known from previous measurements [10,11] and should, in principle, be more easily determined because of the absence of the 14-MeV neutron background of the ${}^3\text{H}(d,\alpha)n$ reaction, we chose to determine the cross-section ratio for ${}^3\text{H}(d,\gamma){}^5\text{He}$ relative to ${}^3\text{H}(d,\alpha)n$ by comparison with the ratio for ${}^2\text{H}({}^3\text{He},\gamma){}^5\text{Li}$ relative to ${}^2\text{H}({}^3\text{He},\alpha){}^1\text{H}$.

*Now at XonTech, Inc., Van Nuys, CA 91406.

†Now at EGG-Astrophysics Research Corp., Long Beach, CA 90801-5709.

II. EXPERIMENTAL DETAILS

The ${}^3\text{H}(d,\gamma){}^5\text{He}$ and ${}^3\text{H}(d,\alpha)n$ reactions were studied by bombarding a tritiated-titanium target with a deuteron beam produced by the model-JN Van de Graaff accelerator in the Alfred P. Sloan Laboratory at the California Institute of Technology. The mirror reactions were studied by bombarding a deuterated-titanium target with a ${}^3\text{He}$ beam from the JN.

A schematic diagram of the target and detector arrangement is shown in Fig. 1. Alpha particles were detected in a surface barrier detector located at an angle of 150° relative to the beam direction. A $2\text{-}\mu\text{m}$ -thick Cu foil was placed in front of the detector to stop elastically scattered beam particles. Gamma rays were detected in a NaI pair spectrometer located 68.6 cm from the target at an angle of 0° relative to the beam direction. Backgrounds from neutron-induced reactions were greatly reduced by the coincidence requirements of the pair spectrometer, by restrictive collimation between the target and detector, and by the use of a low-mass target, as described below. Separate target chambers were used for the ${}^3\text{H}(d,\gamma){}^5\text{He}$ and ${}^2\text{H}({}^3\text{He},\gamma){}^5\text{Li}$ runs in order to avoid any tritium cross contamination. The two chambers were alike except for an additional 5-cm distance between the target and α -particle detector in the tritium target chamber.

The pair spectrometer consisted of an array of seven hexagonal NaI detectors arranged in a honeycomb pattern (six around one). Each detector was 15.24 cm long

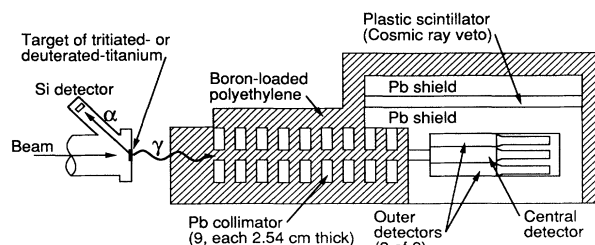


FIG. 1. Schematic diagram of the target and detector arrangement.

and 3.2 cm wide (face to face) and had a resolution of 13% for 0.511-MeV gamma rays. Lead collimators with an inner diameter of 2.54 cm prevented gamma rays from the target from reaching the outer detector directly. Signals from the central detector were gated so that only pair production events would be counted. The gate was derived from a triple coincidence between the signals from two outer detectors and the central detector. The three signals were required to occur within 30 ns, and the signals from the outer detectors were required to be between 0.43 and 0.60 MeV. This energy window was set by using a ^{22}Na source, and the detection system was extensively tested by measuring gamma rays from $^{19}\text{F}(p,\alpha\gamma)^{16}\text{O}$ and $^3\text{H}(p,\gamma)^4\text{He}$. [For the $^3\text{H}(p,\gamma)^4\text{He}$ runs, the detector was placed at 45° relative to the beam, because these gamma rays emitted with a $\sin^2\theta$ distribution.]

The entire detector assembly was shielded by 10 cm of lead and at least 10 cm of boron-loaded polyethylene. In addition, 58 cm of polyethylene was interposed between the target and central detector. This reduced the incident neutron flux by about a factor of 500 while reducing the incident gamma flux by about a factor of 3. Paddles of plastic scintillator 1.57 cm thick were placed over the top and sides of the detector within the lead shield to detect and veto cosmic-ray events.

For the $^3\text{H}(d,\gamma)^5\text{He}$ run, the target consisted of about 2 Ci of tritium absorbed in a 4-mg/cm² layer of titanium which had been evaporated onto a beryllium disk 0.025 cm thick and 1.9 cm in diameter. For the $^2\text{H}(^3\text{He},\gamma)^5\text{Li}$ run, the same kind of target was used, but the titanium was saturated with deuterium. For both runs the target was mounted on an aluminum vacuum barrier 0.025 cm thick. This target design was chosen to reduce the number of high-energy gamma rays produced by secondary (n,γ) reactions in and near the target in the $^3\text{H}(d,\gamma)^5\text{He}$ run. It should be noted that the Q value for neutron capture on a wide range of nuclei is 6–8 MeV and that the cross section for the capture of 14-MeV neutrons may be significant for many nuclei due to the giant electric dipole resonance [12]. Gamma rays mainly from 14-MeV-neutron capture reactions in and near the target must therefore be considered as a possible source of background for all experiments of this type. Furthermore, this source of background cannot be removed with conventional time-of-flight methods, which use beam pulses of about 1 ns duration.

In order to further decrease the background of high-energy gammas from neutron-induced reactions in the target area, a series of lead collimators was used to restrict the region of the target chamber viewed by the detector to a 4-cm-diam circle centered on the target. The walls of the target chamber were located outside of this region. In addition, the chamber and its flanges were constructed entirely of aluminum, which has a lower cross section for background (n,γ) reactions than iron or copper [13].

With these background-reduction techniques in effect, the most important remaining source of background is high-energy gamma rays produced by neutron-induced reactions in the central NaI detector itself. This back-

ground could be rejected by using time-of-flight techniques. However, it was found to be impractical to obtain a pulsed beam from the JN accelerator on the short beam line on this accelerator. Pulse-shape discrimination techniques, such as those used by Cecil and Wilkinson [1], were also tested, as was the use of BGO instead of NaI as the central detector, but neither of these strongly reduced the remaining background. It was therefore decided to proceed with the experiment as described above and to study the response of the detector to both signals and backgrounds by measuring gamma-ray spectra from $^{19}\text{F}(p,\alpha\gamma)^{16}\text{O}$, $^3\text{H}(p,\gamma)^4\text{He}$, $^2\text{H}(^3\text{He},\gamma)^5\text{Li}$, and $^3\text{H}(d,\gamma)^5\text{He}$ and by performing Monte Carlo calculations.

The measurements for $^3\text{H}(d,\gamma)^5\text{He}$ were obtained in a 33-h run using a 0.8- μA molecular beam of deuterium ($^2\text{H}_2^+$). The beam energy was chosen to obtain 100-keV effective energy per deuteron in the target. The effective energy was determined from the thick-target yields of α particles from $^3\text{H}(d,\alpha)n$. With this beam current, the total “single” count rate in the central detector was about 2 kHz, and pulse pileup and electronic dead time were negligible. The measurements for $^2\text{H}(^3\text{He},\gamma)^5\text{Li}$ were obtained immediately after the $^3\text{H}(d,\gamma)^5\text{He}$ measurements in a 21-h run with a 4.5- μA $^3\text{He}^+$ beam current. Higher beam currents were possible because backgrounds were lower for this reaction. The effective ^3He beam energy was set to 600 keV (equivalent to 400 keV deuteron ener-

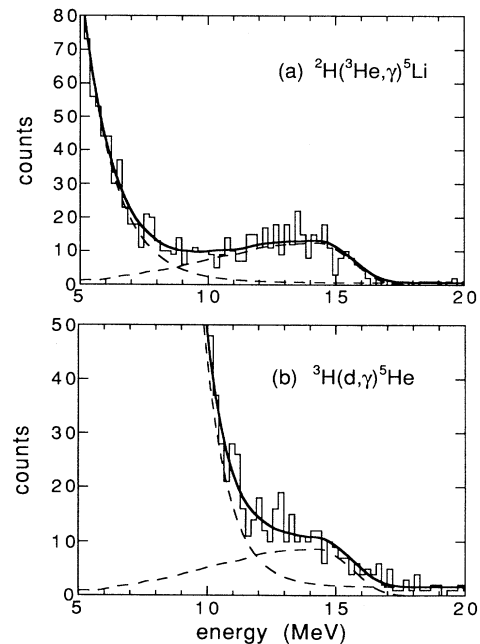


FIG. 2. Triple-coincidence spectra obtained with the pair spectrometer for the (a) $^2\text{H}(^3\text{He},\gamma)^5\text{Li}$ and (b) $^3\text{H}(d,\gamma)^5\text{He}$ runs. The curves through the data are peak fits obtained using the maximum-likelihood method of Aways [24]. The same peak shapes were used for gamma rays from $^2\text{H}(^3\text{He},\gamma)^5\text{Li}$ and $^3\text{H}(d,\gamma)^5\text{He}$. The exponential background in (a) is due mainly to gamma rays generated by 15-MeV protons in the target; in (b) it is due mainly to gamma rays generated by 14-MeV neutrons in the NaI detector.

gy in the center-of-mass system), slightly below the peak of the broad resonance in ${}^3\text{He}(d,p){}^4\text{He}$. The resulting spectra are shown in Fig. 2. During these runs, the energy windows for 0.511-MeV annihilation quanta in the outer detectors were checked several times using a ${}^{22}\text{Na}$ source and were found to remain constant. Aside from these checks, the detector and electronics were not disturbed in any way in these two runs. It is therefore assumed that the efficiency of the pair spectrometer was the same for the ${}^3\text{H}(d,\gamma){}^5\text{He}$ and ${}^2\text{H}({}^3\text{He},\gamma){}^5\text{Li}$ runs.

III. MONTE CARLO CALCULATIONS OF THE DETECTOR RESPONSE

Measured triple-coincidence spectra for the ${}^{19}\text{F}(p,\alpha\gamma){}^{16}\text{O}$ and ${}^3\text{H}(p,\gamma){}^4\text{He}$ reactions are shown in Fig. 3 along with predictions for these spectra obtained with the Monte Carlo code EGS4 (electron-gamma shower, version 4) [14], which simulates the coupled transport of electrons and photons in an arbitrary geometry. In these calculations a point source of monochromatic gamma rays was considered to be at the center of the target. Each gamma ray and each secondary electron or photon generated in the subsequent shower was transported until the particle energy was below a cutoff value (10 keV for photons, 100 keV for electrons) or until the particle reached the boundary of the problem. Energy deposited in the central detector was accumulated in a spectrum, subject to the triple-coincidence requirements. The predicted spectrum was folded with the detector-response function using the method of Berger and Seltzer [15]. The resulting predictions for the two reactions have been normalized to have the same integral as the mea-

sured spectra. The predicted peak shapes compare well with the measured ones. The success of this Monte Carlo model gives us confidence that we can accurately predict pulse-height distributions for gamma rays over this energy region.

Calculations of the response of the pair spectrometer to gamma rays from ${}^2\text{H}({}^3\text{He},\gamma){}^5\text{Li}$ were also performed with EGS4. The incident gamma rays were presumed to be distributed as in the spectrum determined by Buss *et al.* [10] for this reaction. The results of Buss *et al.*, corrected for detector resolution, are reproduced in Fig. 4. There are two components in the spectrum: a high-energy peak, corresponding to decay directly to the ground state of ${}^5\text{Li}$, and a lower-energy peak due to decay through the broad first excited state. EGS4 calculations were performed for the two components separately; the results for the triple-coincidence spectra are shown in Fig. 5. The detector was not expected to resolve the two components.

In order to understand detector backgrounds better for the ${}^3\text{H}(d,\gamma){}^5\text{He}$ runs and to determine if longer runs would significantly improve the results, calculations of the response of the detector to gamma rays from ${}^3\text{H}(d,\gamma){}^5\text{He}$ and from background (n,γ) reactions were performed using the Monte Carlo code COG [16] in combination with EGS4. Both programs were needed, because COG transports neutrons and gamma rays, while EGS4 transports gamma rays and electrons. The geometry of the problem was specified in detail using the generalized COG geometry package. For the ${}^3\text{H}(d,\gamma){}^5\text{He}$ calculations, an isotropic point source of gamma rays, distributed as in Fig. 4, was placed at the center of the target. The energy deposited in the central detector of the pair spectrometer with and without the coincidence requirements was calculated using EGS4. For the neutron-induced background reactions, an isotropic source of 14-MeV neutrons was generated at the target. Each neutron was transported by COG until it was removed by an interaction or reached the boundary of the problem. Any gamma ray that was generated by a neutron during this process was transported by EGS4. The cross sections used by COG were taken from the Evaluated Nuclear Data Library [17]. Because of a lack of data, we estimated the cross section for ${}^{127}\text{I}(n,\gamma)$ for $E_\gamma > 12$ MeV from the ${}^{208}\text{Pb}(n,\gamma)$ predictions of Reffo *et al.* [18] by using the

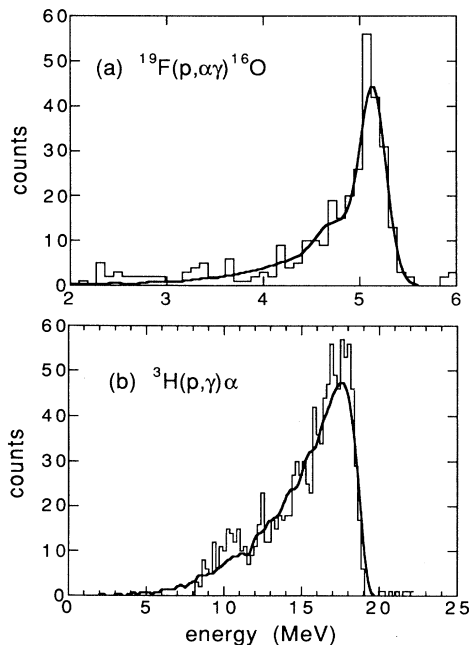


FIG. 3. Triple-coincidence spectra obtained with the pair spectrometer for (a) ${}^{19}\text{F}(p,\alpha\gamma){}^{16}\text{O}$ at $E_p = 365$ keV and (b) ${}^3\text{H}(p,\gamma){}^4\text{He}$ at $E_p = 800$ keV. The curves through the data are Monte Carlo predictions obtained with EGS4.

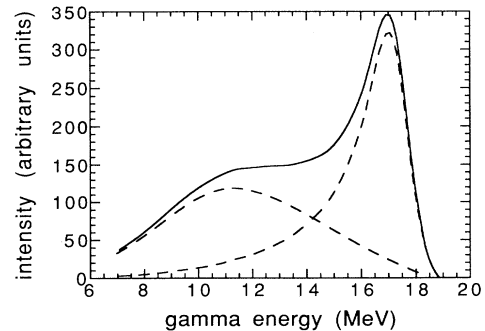


FIG. 4. Gamma rays emitted by ${}^2\text{H}({}^3\text{He},\gamma){}^5\text{Li}$ as determined by Buss *et al.* [10]. The solid curve is the sum of the two dashed curves.

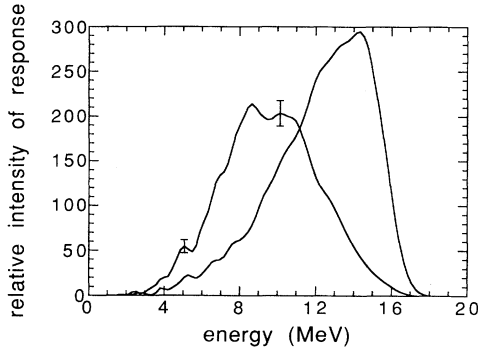


FIG. 5. Monte Carlo prediction of triple-coincidence spectra for the two components of the spectrum shown in Fig. 4. For each component, 200 000 gamma rays were incident on the central detector. The error bars denote typical statistical uncertainties in these predictions.

dipole sum rule [12] and correcting for the Q -value difference. The results for the ${}^3\text{H}(d,\gamma){}^5\text{He}$ signal and neutron-induced backgrounds are shown in Fig. 6. These predictions were obtained without the requirement of triple coincidence; the results obtained with triple coincidence are similar, but have larger statistical uncertainties. The results of these calculations are consistent with our observations that the background is close to exponential in shape over the energy range covered by the present experiment. Although the backgrounds are significant, these calculations suggest that the ${}^3\text{H}(d,\gamma){}^5\text{He}$ signal

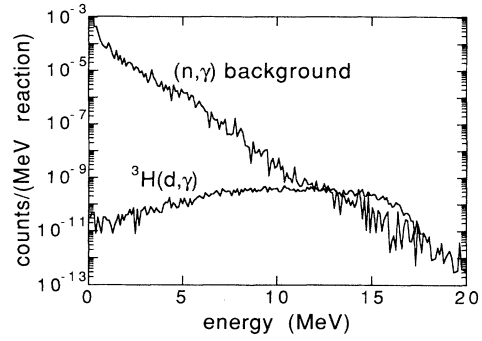


FIG. 6. Monte Carlo prediction of the relative intensities of the ${}^3\text{H}(d,\gamma)$ signal and the neutron-induced backgrounds generated in the central NaI detector when no coincidence requirements are imposed. In the calculation the ${}^3\text{H}(d,\gamma){}^5\text{He}/{}^3\text{H}(d,\alpha)n$ cross-section ratio was taken to be 1×10^{-4} . The structure in the curves is due to statistical fluctuations.

should be observable above about 12 MeV in the spectrum. Furthermore, these calculations show that the difficulty in this experiment is not one of counting statistics, but one of the ratio of gamma signal to neutron-induced background.

IV. DATA ANALYSIS

The yield of gamma rays from ${}^3\text{H}(d,\gamma){}^5\text{He}$ per incident deuteron of energy E_d is given by

$$N_{\gamma}^{\text{DT}}(\theta_{\gamma}) = \epsilon_{\gamma} \Omega_{\gamma} \int_{E_d}^{\infty} \frac{[d\sigma_{\text{DT}\gamma}(E, \theta_{\gamma})/d\Omega_{\text{c.m.}}][d\Omega_{\text{c.m.}}(E, \theta_{\gamma})/d\Omega_{\text{lab}}]f(E)dE}{S_{\text{Ti}}(E) + f(E)S_{\text{H}}(E)}, \quad (1)$$

where $S_{\text{Ti}}(E)$ and $S_{\text{H}}(E)$ are the deuteron stopping powers for titanium and hydrogen, respectively, $f(E)$ is the number ratio of tritium atoms to titanium atoms in the target at a depth corresponding to deuteron energy, E , ϵ is the efficiency of the detector, Ω_{γ} is the solid angle of the pair spectrometer in the laboratory frame of reference, $d\sigma_{\text{DT}\gamma}(E, \theta_{\gamma})/d\Omega_{\text{c.m.}}$ is the differential cross section in the center of mass, and $d\Omega_{\text{c.m.}}(E, \theta_{\gamma})/d\Omega_{\text{lab}}$ is the solid-angle ratio determined by reaction kinematics. The detector efficiency has been removed from the integrand, because in this case it is essentially constant over the small range of deuteron energies in the integral.

A similar expression can be written for the yield of α particles from ${}^3\text{H}(d,\alpha)n$. At low energies the cross section is observed to be isotropic in the center of mass. Therefore we set

$$\begin{aligned} d\sigma_{\text{DT}\alpha}(E, \theta_{\alpha})/d\Omega_{\text{c.m.}} &= \sigma_{\text{DT}\alpha}(E)/4\pi \\ &\equiv \sigma(E)/4\pi. \end{aligned}$$

We define the cross-section ratio $R_{\text{DT}}(E) = \sigma_{\text{DT}\gamma}(E)/\sigma_{\text{DT}\alpha}(E)$ and assume that it is not a function of deuteron energy in the integral. These are good assumptions in this energy region, where the reaction is

dominated by a $J^{\pi} = \frac{3}{2}^{+}$ resonance, and the cross section has been successfully described by a single-level R -matrix analysis [19]. These assumptions may fail at higher energies where direct reactions or higher angular momenta become important. (The measurements of Batay-Csorba for $E_d = 2-12$ MeV cannot be described by pure s waves [7].) With the assumptions we have made, we can write the ratio of the gamma-ray and α -particle yields:

$$\frac{N_{\gamma}^{\text{DT}}(\theta_{\gamma})}{N_{\alpha}^{\text{DT}}(\theta_{\alpha})} = \frac{\epsilon_{\gamma} \Omega_{\gamma} R_{\text{DT}}}{\Omega_{\alpha}} \frac{I^{\text{DT}}(\theta_{\gamma})}{I^{\text{DT}}(\theta_{\alpha})}, \quad (2)$$

where

$$I^{\text{DT}}(\theta_{\gamma}) = \int_{E_d}^{\infty} \frac{\sigma(E)[d\Omega_{\text{c.m.}}(E, \theta_{\gamma})/d\Omega_{\text{lab}}]f(E)dE}{S_{\text{Ti}}(E) + f(E)S_{\text{H}}(E)},$$

and similarly for $I^{\text{DT}}(\theta_{\alpha})$. Note that $I^{\text{DT}}(\theta_{\gamma})/I^{\text{DT}}(\theta_{\alpha}) \neq 1$ in this experiment, because the kinematic solid-angle ratio for gamma rays at 0° is different than that for α particles at 150° . A similar expression can be written for the ratio of gamma-ray to α -particle yields for the ${}^2\text{H}({}^3\text{He}, \gamma){}^5\text{Li}$ run, by assuming that $R_{\text{D}^3\text{He}}(E)$ is not a function of energy in the region of the resonance in ${}^2\text{H}({}^3\text{He}, \alpha){}^1\text{H}$, as seems to be the case.

Taking the ratio of the yield ratios for the two reactions and rearranging terms, one obtains

$$R_{DT} = \frac{N_{\gamma}^{DT}(\theta_{\gamma})}{N_{\gamma}^{D^3\text{He}}(\theta_{\gamma})} \frac{N_{\alpha}^{D^3\text{He}}(\theta_{\alpha})}{N_{\alpha}^{DT}(\theta_{\alpha})} \frac{\Omega_{\alpha}^{DT}}{\Omega_{\alpha}^{D^3\text{He}}} \times \frac{I^{D^3\text{He}}(\theta_{\gamma})I^{DT}(\theta_{\alpha})}{I^{DT}(\theta_{\gamma})I^{D^3\text{He}}(\theta_{\alpha})} R_{D^3\text{He}}. \quad (3)$$

Here we have assumed that the solid angle and efficiency of the pair spectrometer were constant throughout the two runs. We have also assumed that the efficiency of the α -particle detector (essentially unity) was the same for the two runs.

It is straightforward to evaluate the $I(\theta)$ terms. We use the cross sections for ${}^3\text{H}(d,\alpha)n$ given by Hale and Dodder [20], the cross sections for ${}^3\text{He}(d,\alpha){}^4\text{H}$ given by White, Resler, and Warshaw [21], and stopping powers given by Andersen and Ziegler [22]. The solid-angle ratio for the α particles due to reaction kinematics is well known (cf. Ref. [23]). For gamma rays at 0° , it can be shown that $d\Omega_{\text{c.m.}}(E, \theta_{\gamma})/d\Omega_{\text{lab}} = (1+\beta)/(1-\beta)$, where β is the boost from the laboratory to the center-of-mass frame. We use $f(E)=0.3$ for the tritium target and $f(E)=1.9$ for the deuterium target, as determined from thick-target yields of α particles. [Note, however, that the results for R_{DT} are insensitive to the two values of $f(E)$.] For $\theta_{\gamma}=0^\circ$ and $\theta_{\alpha}=150^\circ$, we obtain, for Eq. (3),

$$R_{DT} = \frac{N_{\gamma}^{DT}(0^\circ)}{N_{\gamma}^{D^3\text{He}}(0^\circ)} \frac{N_{\alpha}^{D^3\text{He}}(150^\circ)}{N_{\alpha}^{DT}(150^\circ)} \frac{\Omega_{\alpha}^{DT}}{\Omega_{\alpha}^{D^3\text{He}}} 1.41 R_{D^3\text{He}}. \quad (4)$$

The factor 1.41 is due to the kinematic correction described above. This factor is not unity, because the kinematics are different for a mass-2 beam incident on a mass-3 target and for a mass-3 beam incident on a mass-2 target.

For $R_{D^3\text{He}}$ we use the results of Buss *et al.* [10] for the cross section for ${}^2\text{H}({}^3\text{He},\gamma){}^5\text{Li}$. At 450 keV, Buss *et al.* obtained $21 \pm 4 \mu\text{b}$ for the decay to the ground state with a relative intensity $r=1.00 \pm 0.15$ for the decay to the ground state compared to the decay to the first excited state (see Fig. 4). At 450 keV the evaluation of White, Resler, and Warshaw gives 0.81 ± 0.06 b for the ${}^3\text{He}(d,\alpha){}^4\text{H}$ cross section. Therefore we take $R_{D^3\text{He}} = (5.2 \pm 1.1) \times 10^{-5}$, including decay by both branches, where the uncertainty was obtained from the quadrature sum of the quoted uncertainties.

For the α -particle detectors in this experiment, $\Omega_{\alpha}^{DT}/\Omega_{\alpha}^{D^3\text{He}} = 0.75$. The ratio of the α -particle yields was obtained from the total counts detected by the surface barrier detector for each of the two runs. Since protons from the ${}^3\text{He}(d,p){}^4\text{He}$ reaction were also detected in the ${}^2\text{H}({}^3\text{He},\gamma){}^5\text{Li}$ run, these were subtracted from the total counts to obtain the α -particle yields. We obtain $N_{\alpha}^{D^3\text{He}}/N_{\alpha}^{DT} = 3.0 \pm 0.1$ for the integrated charges, tar-

gets, and solid angles used in this experiment.

The ratio of the gamma-ray yields in Eq. (4) was obtained in a peak-fitting analysis. For the data from both the ${}^2\text{H}({}^3\text{He},\gamma){}^5\text{Li}$ and ${}^3\text{H}(d,\gamma){}^5\text{He}$ runs, the background was represented as a constant-plus-exponential tail, and the same peak shape for decay to the mass-5 ground state was used. (The 0.09-MeV difference between the quoted energies of the second excited states in ${}^5\text{He}$ and ${}^5\text{Li}$ has been ignored, since this is smaller than one energy bin in our data.) The peak shape was determined by fitting the ${}^2\text{H}({}^3\text{He},\gamma){}^5\text{Li}$ data with the two curves of Fig. 5 and by allowing the ratio of the intensities of the two transitions, r , to vary. When a good fit was obtained, r was fixed, and the spectra from both ${}^2\text{H}({}^3\text{He},\gamma){}^5\text{Li}$ and ${}^3\text{H}(d,\gamma){}^5\text{He}$ were fitted. The measured spectra and the corresponding fits are shown in Fig. 2.

The fits shown in Fig. 2 were obtained using the method of maximum likelihood as described by Aways [24]. The well-known χ^2 -fitting method [25] was also used for comparison. The method of Aways is more appropriate in this situation, because the number of counts in the region of interest is small. For the χ^2 -fitting method, it can be shown that the integral of the fitting function is smaller than the integral of the counts by an amount equal to the minimum value of χ^2 . For the method of Aways, the integral of the fitting function is equal to the integral of the counts. Using this method, we obtain $N_{\gamma}^{DT}/N_{\gamma}^{D^3\text{He}} = 0.71 \pm 0.10$, where the uncertainty is defined in the same way as for the χ^2 -fitting method. (For comparison, the χ^2 -fitting method gives $N_{\gamma}^{DT}/N_{\gamma}^{D^3\text{He}} = 0.83 \pm 0.11$.) The best fit was obtained for $r=5 \pm 2$, although all values of $r \geq 2$ are consistent with these data. For $r = \infty$ (no decay to the first excited state), we still obtain a good fit with $N_{\gamma}^{DT}/N_{\gamma}^{D^3\text{He}} = 0.65 \pm 0.09$. Although the quantity r is not well determined by this experiment, we note that the values of r for ${}^2\text{H}({}^3\text{He},\gamma){}^5\text{Li}$ obtained by Buss *et al.* [10] ($r=1.0$) and by Cecil and Wilkinson [1] ($r=0.6$) are not consistent with the value derived from the present data.

V. RESULTS

Our result for the cross-section ratio for ${}^3\text{H}(d,\gamma){}^5\text{He}$ relative to ${}^3\text{H}(d,\alpha)n$ is $R_{DT} = (1.2 \pm 0.3) \times 10^{-4}$, where the uncertainty was obtained by combining the component uncertainties in quadrature and includes the uncertainty in the cross-section ratio for ${}^2\text{H}({}^3\text{He},\gamma){}^5\text{Li}$ relative to ${}^2\text{H}({}^3\text{He},\alpha){}^4\text{H}$. By comparing the mirror reactions, we do not require an ‘‘absolute efficiency’’ for the detector, since it cancels out of Eq. (3) along with solid-angle and transmission factors. An alternative method of analysis would be to determine the detector efficiency with another calibration reaction, which would introduce the uncertainty in that cross section. For example, Cecil and Wilkinson [1] used the ${}^{11}\text{B}(p,\gamma){}^{12}\text{C}$ and ${}^{11}\text{B}(p,\alpha){}^8\text{Be}$ reactions, which introduced a systematic uncertainty of about $\pm 20\%$. The quoted uncertainty in their final result ($\pm 24\%$) is statistical only and does not include this systematic uncertainty. In comparison, our method has provided a smaller overall uncertainty and has the distinct advantage of utilizing the correct peak shape. Yet another

er alternative method of analysis is that used by Morgan *et al.* [2], who used Monte Carlo techniques to predict the product of the detector efficiency, solid angle, and transmission to about $\pm 10\%$. In our experiment a similar calculation with an uncertainty of $\pm 15\%$ would reduce the final uncertainty to about $\pm 20\%$. Thus a slight improvement in uncertainty might be possible, but might be difficult to justify in this experiment, because of the relatively poor signal-to-background ratio.

A more significant improvement to this experiment would be the use of time-of-flight techniques [2,7]. As noted above, this was found to be impractical on the short beam line on the JN accelerator, and support and manpower limitations prevented us from moving our experiment to a low-energy facility with pulsed beam. Thus, although our experiment provided a measurement with uncertainties comparable to experiments performed with different techniques, extended measurements with the present technique were deemed unwarranted. A truly definitive measurement of the cross section for ${}^3\text{H}(d,\gamma){}^5\text{He}$ relative to ${}^3\text{H}(d,\alpha)n$ would require a reduction of backgrounds sufficient to observe distinctly the gamma rays from both the decays to the ground state and to the broad first excited state of ${}^5\text{He}$.

Figure 7 shows a comparison of our result with previous results. Our result for R_{DT} is larger than those of Morgan *et al.* [2] and Cecil and Wilkinson [1], although an important difference in the definition of these results should be noted. Both Morgan *et al.* and Cecil and Wilkinson state that their results are for the decay to the ground state only. Our result includes contributions from decays to both the ground state and first excited state in ${}^5\text{He}$, although the former was found in our measurement to dominate the latter. This difference in definition could account for part of the difference between the results. It seems clear that the spectra of the gamma rays from the decays to the ground state and first excited state are both rather broad and overlap one another. Therefore it is important to specify the spectral

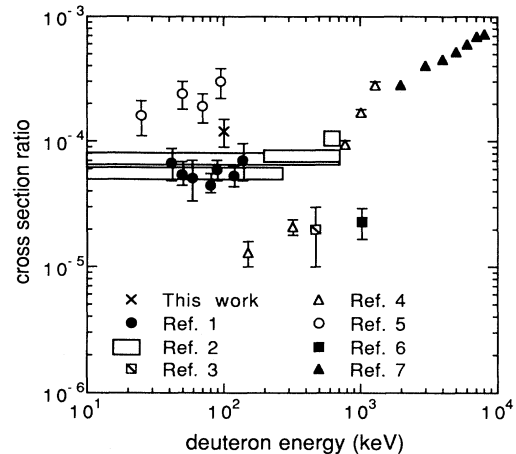


FIG. 7. Summary of measured values of the cross-section ratio ${}^3\text{H}(d,\gamma){}^5\text{He}/{}^3\text{H}(d,\alpha)n$.

fraction assumed in any experiment that measures or utilizes these cross-section ratios.

ACKNOWLEDGMENTS

We thank the staff of the W.K. Kellogg Laboratory at the California Institute of Technology for their help and support of this experiment. Special thanks are extended to A. Rice and S. Stryker of the Alfred P. Sloan Laboratory for maintenance of the JN accelerator and to G. Wells and D. Morgret of Lawrence Livermore National Laboratory for development of the beam line and electronic systems. We also thank B. Remington and M. Pitt for their help in the early stages of this experiment. This work was performed in part under the auspices of the U.S. Department of Energy by the Lawrence Livermore National Laboratory under Contract No. W-7405-ENG-48 and supported in part at the California Institute of Technology by the National Science Foundation, Grant No. PHY88-17296.

- [1] F. E. Cecil and F. J. Wilkinson III, *Phys. Rev. Lett.* **53**, 767 (1984).
- [2] G. L. Morgan, P. W. Lisowski, S. A. Wender, Ronald E. Brown, Nelson Jarmie, J. F. Wilkerson, and D. M. Drake, *Phys. Rev. C* **33**, 1224 (1986).
- [3] J. H. Coon and R. W. Davis, *Bull. Am. Phys. Soc.* **4**, 366 (1959) (abstract only).
- [4] W. Buss, H. Waffler, and B. Ziegler, *Phys. Lett.* **4**, 198 (1963).
- [5] V. M. Bezotosnyĭ, V. A. Zhmaĭlo, L. M. Surov, and M. S. Shvetsov, *Yad. Fiz.* **10**, 225 (1969).
- [6] A. Kosiara and H. B. Willard, *Phys. Lett.* **32B**, 99 (1970).
- [7] P. A. Batay-Csorba and C. A. Barnes, *Bull. Am. Phys. Soc.* **20**, 829 (1975) (abstract only); P. A. Batay-Csorba, Ph.D. thesis, California Institute of Technology, 1975.
- [8] J. C. Riley, H. R. Weller, and D. R. Tilley, *Phys. Rev. C* **40**, 1517 (1989).
- [9] F. Ajzenberg-Selove, *Nucl. Phys.* **A490**, 1 (1988).
- [10] W. Buss, W. Del Bianco, H. Waffler, and B. Ziegler, *Nucl. Phys.* **A112**, 47 (1968).
- [11] F. E. Cecil, D. M. Cole, R. Philbin, Nelson Jarmie, and Ronald E. Brown, *Phys. Rev. C* **32**, 690 (1985).
- [12] I. Bergqvist, in *Neutron Radiative Capture*, edited by R. E. Chrien (Pergamon, New York, 1984), p. 33.
- [13] J. Kantele and M. Valkonen, *Phys. Lett.* **39B**, 625 (1972), and references therein.
- [14] Walter R. Nelson, Hideo Hirayama, and David W. O. Roger, Stanford Linear Accelerator Report No. SLAC-265, 1985.
- [15] M. J. Berger and S. M. Seltzer, *Nucl. Instrum. Methods* **104**, 317 (1972).
- [16] Thomas P. Wilcox, Jr. and Edward M. Lent, Lawrence Livermore National Laboratory Report No. M-221-1, 1989.
- [17] R. J. Howerton, R. E. Dye, and S. T. Perkins, Lawrence Livermore National Laboratory Report No. UCRL-50400, Rev. 1, 1981.
- [18] G. Reffo, M. Blann, and B. A. Remington, *Phys. Rev. C* **38**, 1190 (1988); M. Blann, Lawrence Livermore National Laboratory Report No. UCRL-100324, 1989.

- [19] Nelson Jarmie, Ronald E. Brown, and R. A. Hardekopf, *Phys. Rev. C* **29**, 2031 (1984).
- [20] G. M. Hale and D. C. Dodder, in *Nuclear Cross Sections for Technology*, Natl. Bur. Stand. (U.S.) Spec. Publ. No. 594, edited by J. L. Fowler, C. H. Johnson, and C. D. Bowman (U.S. GPO, Washington, D.C., 1980), p. 650.
- [21] Roger M. White, David A. Resler, and Stephen I. Warshaw, in *Proceedings of the International Conference on Nuclear Data for Science and Technology*, Julich, Federal Republic of Germany, 1991, edited by S. M. Qaim (Springer-Verlag, New York, 1991), p. 834.
- [22] H. H. Andersen and J. F. Ziegler, *Hydrogen Stopping Powers and Ranges in All Elements* (Pergamon, New York, 1977), p. 16.
- [23] J. B. Marion and F. C. Young, *Nuclear Reaction Analysis* (North-Holland, Amsterdam, 1968), p. 141.
- [24] Takashi Awaya, *Nucl. Instrum. Methods* **165**, 317 (1979).
- [25] Philip R. Bevington, *Data Reduction and Error Analysis for the Physical Sciences* (McGraw-Hill, New York, 1969), p. 204.